# Automatization of theoretical kinetic data generation for tabulated TS models building - Part II: 1,2 to 1,5-H-shift reactions in alkyl radicals

F.C. Destro, R. Fournet, R. Bounaceur, V. Warth, P.A. Glaude, B. Sirjean

Manuscript prepared for *Combustion and Flame*

# Automatization of theoretical kinetic data generation for tabulated TS models building:

## Part II: 1,2 to 1,5-H-shift reactions in alkyl radicals

**Authors: F.C. Destro[1], R. Fournet[1], R. Bounaceur[1], V. Warth[1], P.A. Glaude[1], B. Sirjean[*1]**

[1]***Laboratoire Réactions et Génie des Procédés, Université de Lorraine, CNRS, LRGP, F-54000 Nancy, France***

*Corresponding author(s): **Baptiste Sirjean baptiste.sirjean@univ-lorraine.fr**

## Abstract

Branched alkanes make up a significant fraction of sustainable alternative fuels. The accurate chemical kinetic modeling of the pyrolysis and oxidation of those fuels requires the availability of accurate kinetic data for branched structures. The accurate theoretical calculation of these data for substituted cyclic transition states (TS) is a challenge because of the large number of configurations that can be created, especially in the larger TS cycles. These configurations originate from all the possible combinations of the orientations of the substituents (axial or equatorial) on the cyclic TS and diastereomers in the reactants, which makes the rigorous counting of the multiple parallel pathways complicated. In this paper, the isomerisation reactions of branched alkyl radicals are theoretically investigated using the code presented in the Part I of this paper series. The 1,2 to 1,5-H-shift reactions are studied within the tabulated transition state models approach, where chain substituents are represented by methyl groups, and all combinations of substitutions in the model TSs are included in a table with their computed rate constants. The rate constants computed for hundreds of reactions with our code demonstrate the necessity to consider all the TS configurations in order to get accurate data. The presence of spectator substituents in the cyclic transition state is shown to have a major impact on the rate constants, increasing their values by more than a factor of 10 for some cases. The tabulated TS models (TMTS) method is validated by comparisons with available experimental data in the literature and is one of the only approach able to accurately capture the impact of branching on the rate constants of isomerizations for large alkyl radicals, which are still difficult to calculate with high-level on-the-fly ab initio calculations.

*Keywords: Automatic kinetic rates, branched alkanes, H-shift reactions, Tabulated Models of Transition State*

## Novelty and Significance

The work presented here is the second part of a study describing the application of a code for generating accurate kinetic rates of branched alkyl radicals isomerisations (H-shifts). The code enabled the calculation of rate constants for all combination of branched alkyl structures submitted to isomerisations involving 3 and 6 membered-ring transition states. This code is the first one that considers multiple transition state cyclic configuration (axial and equatorial position of substituents), which is a key feature when calculating accurate rate constants for branched alkyl structures. The results showed an important impact of the branching in the kinetic rates, with changes of more than an order of magnitude in the kinetic isomerisations for linear and branched structures. A complete table of transition state models for 1,2 to 1,5 H-shift reactions is provided, which can be used to improve the current kinetic data used in branched alkane mechanisms.

**Authors Contributions**

F.C. Destro: data curation, formal analysis, writing (original draft);
R. Fournet: supervision, writing (review and editing);
R. Bounaceur: software, methodology;
V. Warth: software, methodology;
P.A. Glaude: supervision, writing (review and editing);
B. Sirjean: funding acquisition, supervision, writing (review and editing).

## 1. Introduction

Combustion systems are the main source of energy production in the world, however, they are mostly fed by fossil-based fuels, which impact directly the environment by producing greenhouse gases and contributing to global warming. An emerging alternative to fossil fuels is the bio-based fuels that are produced from biomass and reduce the carbon footprint of combustion by closing the carbon cycle. These alternative fuels are similar to fossil fuels and their storage, transport, and use are close to the ones applied in the current combustion systems [1,2]. However, they present new challenges, as the mixture of chemical compounds changes drastically with the biomass source and can impact the combustion performance, fuel storage, and formation of pollutants [2,3].

For the three main classes of fuels in transportation, there are different bio-based alternatives: for gasoline, ethanol from vegetable biomass is the traditional fuel substitute and blend, with a much higher oxygen content than the fossil fuel [3]. The development of longer and more branched alcohol alternatives to ethanol has been studied as an option to increase the energy density and octane number of this alternative fuel [4]. Biodiesel, on the other hand, is mainly produced from vegetable oils or animal fat and is composed mainly of methyl esters of long straight-chain fatty acids [5]. Minor branched components are also present in petro and biodiesel and, even though they may deteriorate the cetane number, they are essential for the cold flow properties [6].

The alternative for jet fuels, called Sustainable Aviation Fuels (SAF), are produced by multiple routes and classified according to this aspect [7]. The first approved petrol alternative jet fuel for blending in commercial use was the Fischer-Tropsch (FT)

Kerosene by Sasol, in 1999 [8]. This class of fuel is mostly formed by iso-paraffins with one or two methyl groups on straight-chain alkanes [8,9], they are usually produced from coal or natural gas, even if bio material can also be used as feedstock. The second most important alternative jet-fuels class, Hydroprocessed Esters and Fatty Acids (HEFA), produced from the hydrotreatment and cracking of plant oil or fatty wastes, presents a considerable percentage of iso-paraffins [10]. The Alcohol-To-Jet fuel (ATK) and Synthetized iso paraffins (SIP) are also two important classes of bio-based alternative for jet fuels with a high presence of highly branched alkanes, with presence of components such as 2,2,4,6,6-pentamethylheptane, 2,2,4,4,6,8,8-heptamethylnonane, and farnesane (2,6,10-trimethyldodecane) [10,11].

The presence of branching compounds on different types of fuels impact their combustion characteristics, such as ignition delay time, laminar burning velocity [11,12], and particle emissions [13], as well as their liquid phase properties [14–16]. The advent of new alternative fuels with new chemical composition, increases the demand of more accurate chemical models for the prediction and comprehension of the mechanisms implicated in the oxidation and pyrolysis of these new compounds, in particular for branched hydrocarbons.

Reaction mechanisms describing the chemical decomposition and combustion of fuels generally contains hundreds or even thousands of species and reactions. For each chemical reaction, an accurate description of the reaction rate is essential to proper reproduce the combustion characteristics [17]. Usually, the kinetic data for most important reactions are obtained by experimental measures or theoretical calculations,

and, when a value for a given reaction is not readily available, it is estimated by similarities with well-known kinetic rates [18].

At high temperatures or in the absence of oxygen, the main components of fuels and bio-based fuels, n-alkanes and iso-alkanes, decompose forming alkyl radicals that are submitted to unimolecular reactions, i.e. β-scission and internal hydrogen migration. The latter reaction class, also called H-shift reactions, are of major importance as they change radical position on the chains [19,20].(add ref construction pag)

The internal hydrogen migration reactions in linear alkyls were broadly studied in pyrolysis experiments [21–31], however, measurements for longer and branched alkyl chains are scarce as they decompose by reactions with common products that overlap and difficult the calculation of separated rates, as it was noticed in Tsang et al. shock tube study of heptyl radicals [32]. Two studies from McGivern et al. [33] and Awan et al. [34] used single pulse shock tube experiments to determine H-shift reaction rate constants on 4-methyl-1-pentyl and 5-methyl-1-hexyl radicals, respectively. Both studies agreed that the presence of methyl groups on the radical chain led to higher isomerisation rates, hence the analogy with reactions of straight chain alkyls was found to not properly describe those reaction coefficients.

Theoretical studies of these reactions were also performed mostly for linear alkyl chains [35–40]. Davis and Francisco performed theoretical studies using the CBS-Q, G2 and G4 composite methods [41–43]. They observed a minor impact of the abstracted site location relative to the terminal carbon on the rate constants. On the other hand, their results indicated an important effect of the branched positions on the TS cycle (equatorial and

axial) on the rate coefficients, as well as a major effect of diaxial interaction on the activation energy of these reactions. In 2014, Wang et al. [44] combined transition state theory and the CBS-QB3 composite method to derive reaction rate rules for this reaction class based on three reaction aspects: the size of the transition state ring, the radical nature of the reactant, and the abstraction site. They derived the rate rules from a combination of similar reactions of straight and branched alkyl chains.

In a recent study from our group [45], the impact of branching of alkyl chains on the rate rules approach was investigated using theoretical calculations. It was found that the size of the substituents had a low effect on the rate constants, but the presence of branching on the alkyl chains was found to increase the rate coefficients by more than a factor of 12 for some highly branched structures. As an alternative to the rate rules, the use of tabulated models of transition states (TMTS) was proposed for 1,3 and 1,4 – H-shift reactions. These models consist in tables of transition states types, containing the description of all combinations of substituents in the TS structure, along with the corresponding modified Arrhenius parameters that can be directly applied in reaction mechanisms. The presence of branching in the alkyl chains can create multiple transition state configurations (as the relative positions of the substituents regarding the cycle may vary), as well as the appearance of multiple reactants and products diastereoisomers.

This behaviour leads to a high number of structures to be build, treated and sorted, which is repetitive and error-prone when performed manually. For this reason, a code was developed by our group to automatically create the branched alkyls, launch the necessary electronic and transition state theory calculations, and organize the resultant rate

constants in tabulated transition state models' format. In the first part of this paper series, the code was detailed and tested against human-produced kinetic rates for the 1,3-H-shift reactions. Here, the code is used to derive TMTS tables for 1,2 and 1,5-H-shift reactions that can be readily used in reaction mechanisms for branched hydrocarbons.

## 2. Methodology

The code presented in Part I of this paper was used to automatically create and handle the structures for the rate coefficients of 1,5-H-shift and 1,2-H-shift reactions, at high-pressure limit, for all the combination of branched structures with $R_i$ = H or $CH_3$, as illustrated in H-shift reaction models with 6 and 3 membered-ring transition structuresFigure 1.

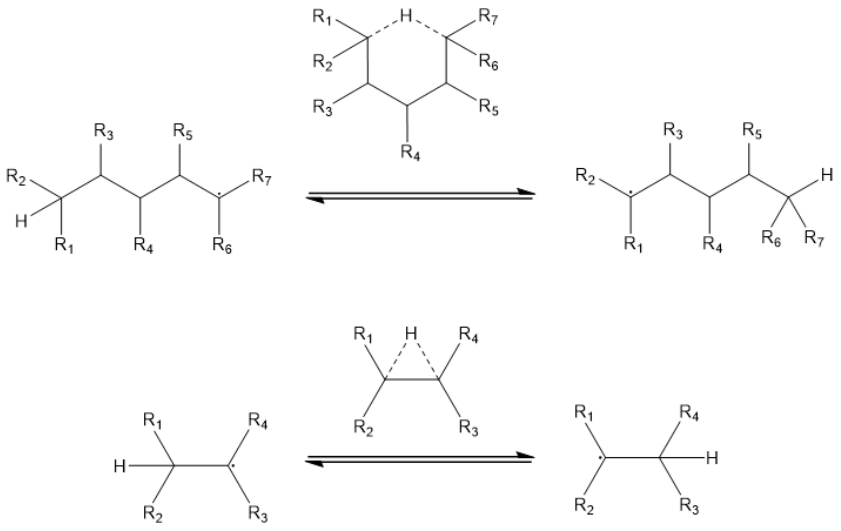


**Figure 1: H-shift reaction models with 6 and 3 membered-ring transition structures**

The methyl substituent was chosen as a generic alkyl chain because, our previous investigations [45] concluded that a methyl could be used to represent a generic alkyl substituent for this reaction class, which was already observed in experimental measurements as well [29].

For the reactions presented here, the kinetic constants were calculated using Canonical Transition State Theory:

$$k(T) = L\kappa(T)\left(\frac{k_b T}{h}\right)\left(\frac{q^{\neq}}{q^R}\right)e^{\left(-\Delta E_0/RT\right)} \quad (1)$$

where L is the statistical factor, $\kappa(T)$ the tunnelling transmission coefficient, $k_b$ the Boltzmann constant, $h$ the Plank constant, $q^{\neq}$ and $q^R$ the partition function of the transition state (TS) and the reactant, respectively, $\Delta E_{0K}$ the difference of energy at 0 K between the TS and the reactant, T the temperature and R the universal gas constant.

The CBS-QB3 method was chosen for all the electronic energies calculations applied in this paper since a previous benchmark from our group [45] showed a good agreement (maximum difference of a factor of 2.1 for temperatures between 500 K and 200K) between the kinetic rates calculated using this method and ANL-F12 reference method [46,47] for the H-shift reactions. The maximum factor of 2.1 is applied in all the kinetic rates curves presented here as the incertitude factor, details are discussed in the supplemental material. The rotational modes were treated as 1D hindered rotors using 1D-HR-U method, and the tunneling effect was included using an Eckart potential. The calculation of rate constants, the hindered rotor, and tunneling treatment was performed using the ThermRot code [48]. All the rate coefficients as a function of the temperature are fitted between 500 and 200 K with a modified Arrhenius. The described calculation steps, from structures generation to TMTS tables building, were all automatically performed by our code detailed in Part I.

When describing the rate parameters in this paper, the nomenclature of Hardwidge is used [21], i.e., an internal hydrogen migration is called using the Ncd format, where N is

the number of atoms in the cyclic TS structured c is the type of radical site in the reactant and d the radical site in the product (p=primary, s=secondary and t=tertiary).

## 3. Results and discussions

### 3.1. Generalities

For the study of 1,5-H-shift reactions as a function of the branching level, a total of 72 possible reactions were identified and launched by the code, which represented 186 reactant structures, 405 transition states, and 114 products. This high number of structures results from the fact that branched structures may present multiple diastereoisomers that must be considered during theoretical calculations for better accuracy, as discussed by David et al. for the cyclic transition states substituents positions divided between axial and equatorial [41,43]. Here, the code goes further for heavily branched structure, as exemplified in Figure 2, for an alkyl containing multiple reactant and transition state configurations.

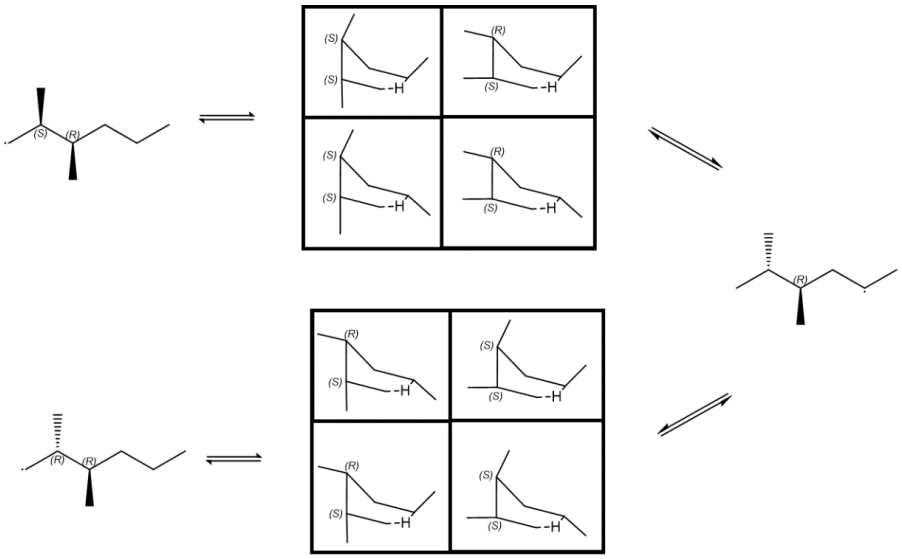

**Figure 2: Example of H-shift reaction with multiple reactant and transition state configurations treated by the code**

The reactants present two chiral centers, leading to two different diastereoisomers (SR and RR structures), each one passing by four transition state configurations and resulting in the same product. The impact of including all the reaction pathways presented in Figure 2 (2 reactants and 8 TS structures with different energies; each reactant and TS has an optical isomer, leading to a total of 4 reactants and 16 TS) on the total rate constant is illustrated in Figure 3.

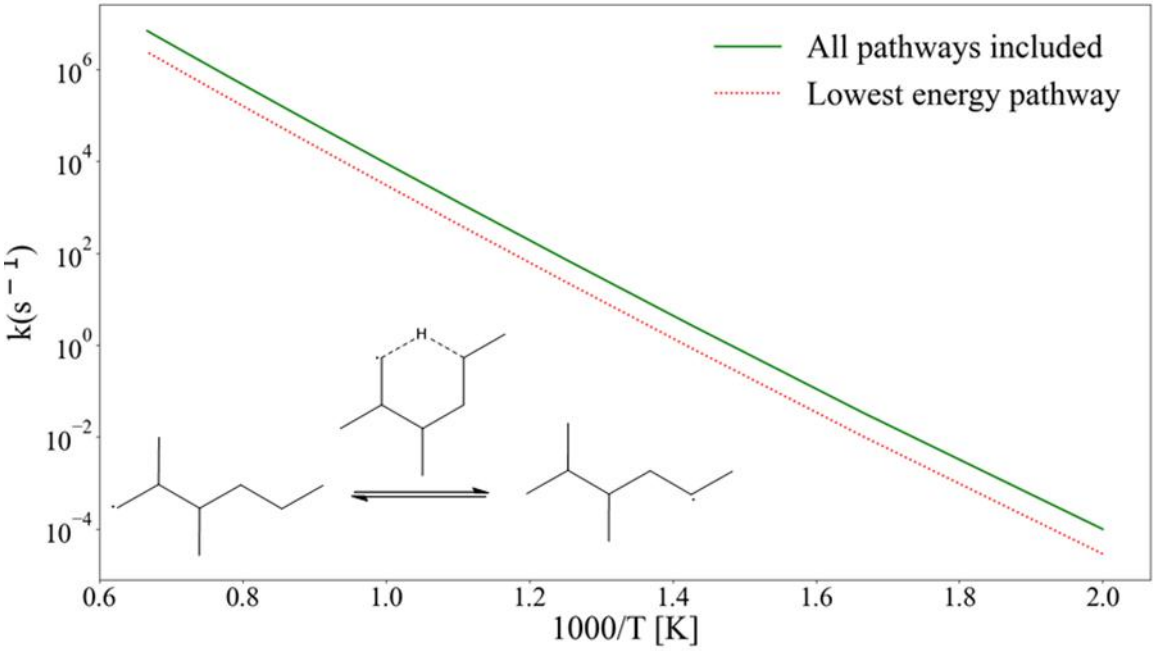


**Figure 3: Rate constants for the reaction of Figure 2, calculated using all pathways (solid line) and only the reactant with lower energy (dotted line).**

Considering only the lowest energy conformer for the reactant and for the transition state structure leads to a rate coefficient 70% lower on average than the rate coefficient that include all the pathways for this specific reaction. The differences in rate coefficients, considering all pathways, increases with the number of transition state configurations.

Usually, the identification and the sorting of multiple reaction pathways are performed manually, and our code was able to implement a sorting and filter algorithm to build all the pathways automatically.

All the calculated high-pressure limit rate constants between 500 and 2000K are presented in Table S1 and Table S2 for the 1,3 and 1,5 H-shift reactions, with their corresponding Arrhenius parameters. An extract of the table is presented in Table 1, for reactions of a primary radical giving primary, secondary, and tertiary radicals (reactions type pp, ps, and pt).

**Table 1: Extract from TMTS Tables, rate constants at different temperatures and their fitted Arrhenius parameters for 1,5-H-shift reactions. The positions of $R_i$ substituents are given in Figure 1.**

| | **reaction type** | | |
|---|---|---|---|
| | **6pp** | **6ps** | **6pt** |
| H-donor Carbon | H, H | $CH_3$, H | $CH_3$, $CH_3$ |
| $R_3$ | H, H | H, H | H, H |
| $R_4$ | H, H | H, H | H, H |
| $R_5$ | H, H | H, H | H, H |
| Carbon radical | H, H | H, H | H, H |
| | | | |
| Temperature (K) | k ($s^{-1}$) | k ($s^{-1}$) | k ($s^{-1}$) |
| 500 | 3.29E+03 | 5.32E+04 | 2.30E+05 |
| 600 | 3.61E+04 | 4.03E+05 | 1.24E+06 |
| 700 | 2.15E+05 | 1.83E+06 | 4.39E+06 |
| 800 | 8.63E+05 | 5.93E+06 | 1.17E+07 |
| 900 | 2.63E+06 | 1.53E+07 | 2.59E+07 |
| 1000 | 6.56E+06 | 3.33E+07 | 4.97E+07 |
| 1100 | 1.42E+07 | 6.41E+07 | 8.62E+07 |
| 1200 | 2.74E+07 | 1.13E+08 | 1.38E+08 |
| 1300 | 4.85E+07 | 1.84E+08 | 2.09E+08 |
| 1400 | 8.02E+07 | 2.82E+08 | 3.00E+08 |
| 1500 | 1.25E+08 | 4.14E+08 | 4.15E+08 |
| **Arrhenius parameters** | | | |

| | | | |
|---|---|---|---|
| A ($s^{-1}$) | 169.3 | 1596.4 | 6069.2 |
| n | 2.39 | 2.16 | 1.89 |
| $E_A$ (kcal/mol) | 11.8 | 9. | 8.10 |

The first part the table includes the description of the substituent presence on different positions of the TS structure. This table can be applied to select rate constants for branched structures in reaction mechanisms.

The rate constants for these three reaction types calculated in this work are presented in Figure 4 together with the computed values proposed by Wang et al. [44].

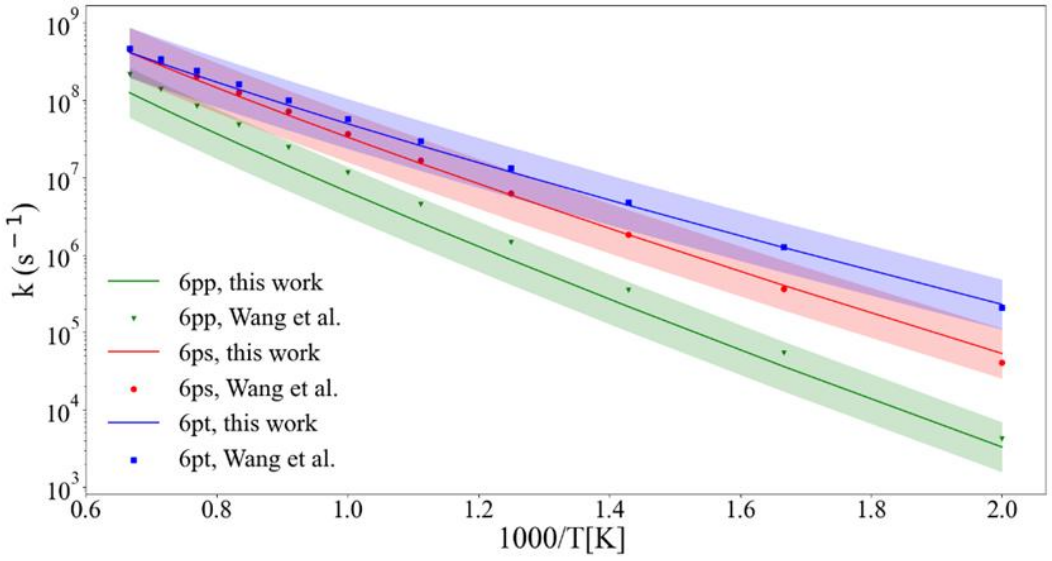


**Figure 4: Reaction rate coefficients for 6px isomerizations, with x = p, s and t. Results from this work (solid lines) and from Wang et al. [44] (symbols). Shaded areas around solid lines correspond to the associated uncertainty.**

A good agreement is observed between our computed kinetic data and those of Wang et al. [44] as the maximum difference is found at 1500K for the 6pp reaction, with our automatic calculated data being 40% lower than the ones from the literature. The behavior of the internal H-transfer is well reproduced in the code-calculated rate constants: the activation energy decreases in the order pp > ps > pt, as more substituted radicals are more stable. In parallel, the preexponential factor increases in the presence of methyl substituents and these two trends accumulate and lead to a major increase in rate constants following the sequence pt > ps > pt, as presented in Figure 4.

The impact of the TS cycle size on the rate constants of internal H-shift reactions is also well established in the literature, with the activation energy decreasing with the ring size from 3 to 6 members in the cycle, because of the decrease in the ring strain. In Figure 5, the rate constants at 500 K of Npp reactions for linear and branched alkyls obtained in the current work together with results of our previous studies [45] are presented.

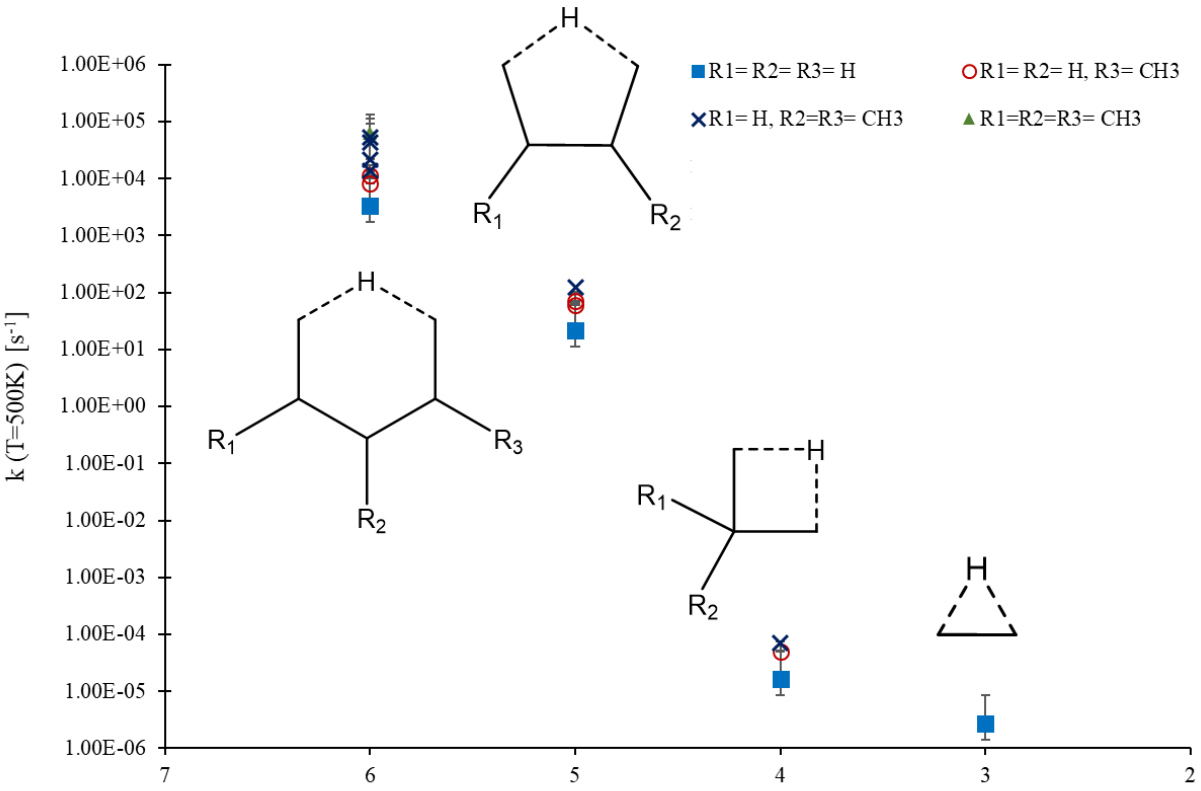


**Figure 5: Rate constants at 500K for pp reactions passing by 6, 5, 4, 3 membered-ring TS, for different levels of branching**

The expected increase in the kinetic data is observed for all the levels of branching on the chain. The results presented in Figure 5 show that as the level of branching increases, the rate constant also increases by more than one order of magnitude for the 6-membered rings. This trend is also observed in smaller cyclic TS structures.

In Figure 6, the activation energies of all the 1,5-H-shift reactions are represented as a function of the reaction enthalpies.

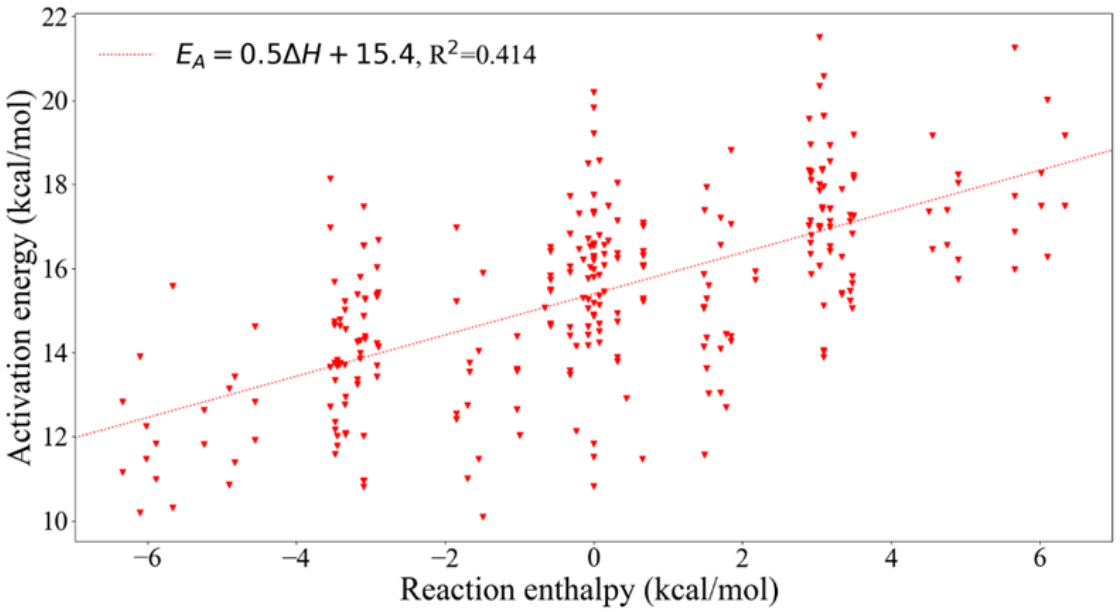


**Figure 6: Evans-Polanyi correlation for 1,5-H-shift activation energies vs reaction enthalpies computed at the CBS-QB3 level of theory.**

Even if there is a tendency to increase activation energy for higher reaction enthalpies, the Evans-Polanyi relationship, which postulates a linear relation between the activation energy and the reaction enthalpy ( $E_A \approx \alpha\Delta H + \beta$), is not appropriate to estimate activation energies for these reactions. This behaviour is explained by the fact that branched alkyls present axial interactions that are relaxed in the transition state cycle, thus the energy difference between reactant and product is not able to express this relaxation, and the deviation is more important for structures with more substituents on the chain. This further reinforces our conclusion that a single rate rule is not appropriate for any degree of branching for an isomerization reaction class and that the TMTS approach for these systems can considerably improve the accuracy of the rate constants over existing correlations.

### 3.2. Validation against literature results

In Figure 7, the automatically calculated kinetic data from this work, for a 6ps reaction with no substituents on the alkyl chain, are compared with experimental data.

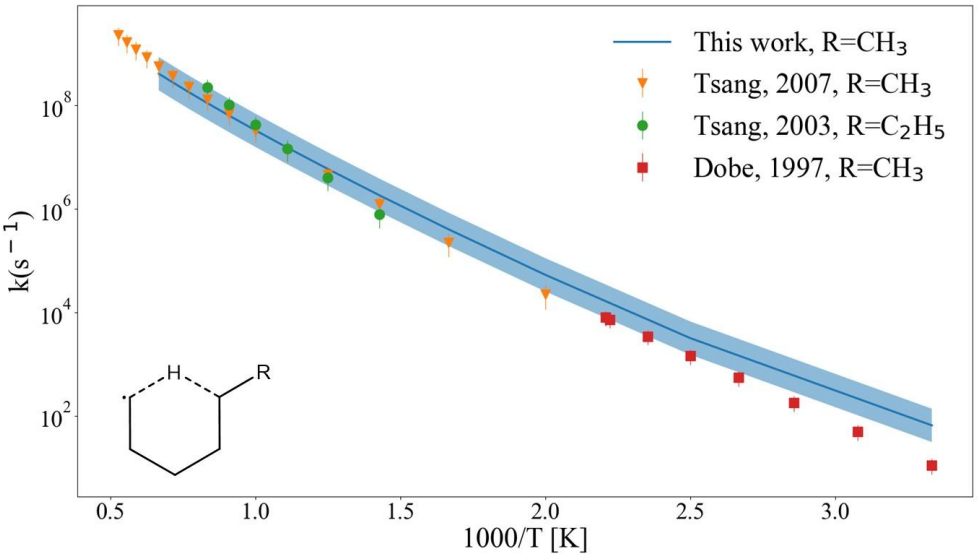


**Figure 7: Reaction rate coefficients for the isomerization of primary linear alkyl radicals into secondary linear alkyl radicals by a 6-membered ring TS, this work (solid line), Tsang, 2007 (▼)[28], Tsang, 2003 (●) [32] and Dobé, 1997 (■)[24].**

Most of the generated kinetic data from our code are in good agreement with experiences, with deviations lower than a factor of 2. The high-pressure rate constants measured by Tsang et al. [32] in 2003 on *n*-hexyl and by Tsang et al. [28] in 2007 on *n*-heptyl corroborate the effectiveness of using a methyl to represent a generic alkyl chain since the coefficients for R=methyl or R=ethyl are indistinguishable within the uncertainty range (i.e. a factor of 1.5 from experimental measurements, mechanisms hypothesis, and high-pressure limit extrapolations). These results were also corroborated by Wang et al.

[44] when studying internal H-migration in alkyl chains. David et al. [41] also calculated internal H-shift reactions in alkyls, and observed that the reactant radical position on the alkyl chain (β or α, i.e. R=$CH_3$ or R=$C_2H_5$) had a minor impact on the rates.

In a previous study [45], our group also investigated the impact of the format and size of alkyl chain substituent in different positions (on the radical carbon, H-transfer carbon, and 'spectator' carbons - carbons on the TS cycle). Both the size and format of substituents were found to have a minor impact on the rate constants from a compensation between a decrease in the activation energy and a decrease in the pre-exponential factor. These studies support the choice of using methyl groups to denote generic alkyl chain substituents in all reactant positions.

The decomposition of branched alkyls was also studied in shock-tube experiments by McGivern et al. [33], who investigated the 4-methyl-1-pentyl radical, and by Awan et al. [34], who focused on 4-methyl-1-hexyl radicals. They extrapolated their measurements by fitting a reaction mechanism, and their results for the isomerizations of alkyl radicals passing by 6-membered rings are compared with the ones automatically calculated in this work in Figures 8 and 9.

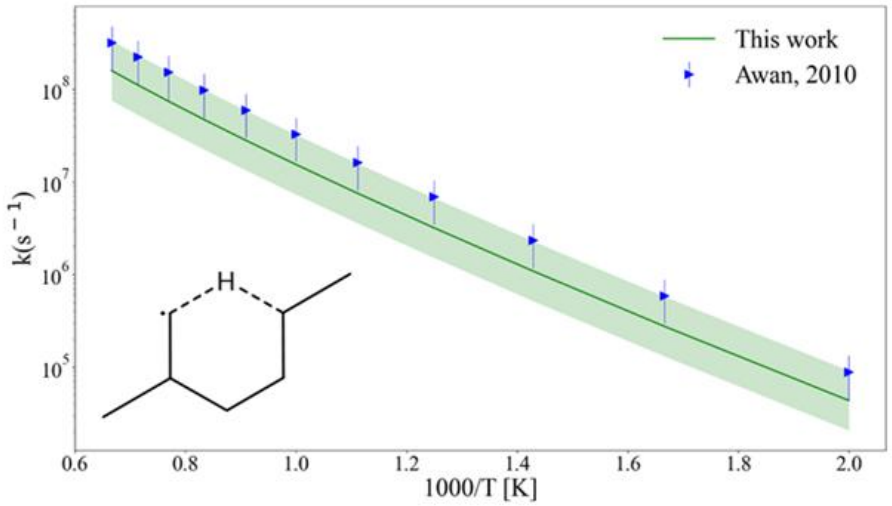


**Figure 8: Rate coefficients for the isomerisation of the 1-hexyl-2-methyl radical obtained in this work (solid line) and extrapolated by Awan et al. (►) [34] .**

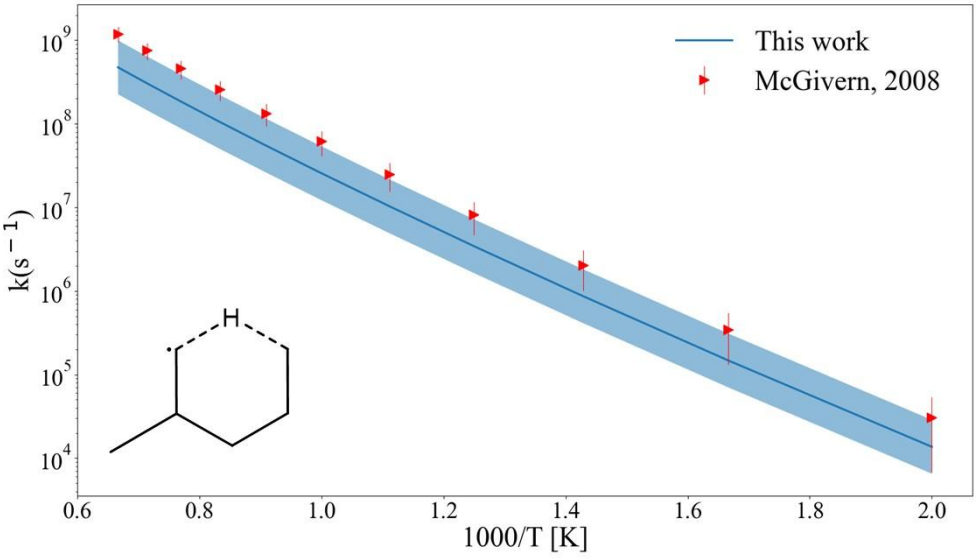


**Figure 9: Reaction rate coefficients for the isomerization of 1-pentyl-4-methyl radical calculated by our code (solid line) and from experimental measurements of McGivern et al. (►) [33].**

The results from this work also confirms another experimental observation from the previous studies: the presence of an alkyl group on the carbon chain increases the rate constants, compared to unsubstituted linear structures. For the alkyls reported here, the rate coefficients were increased by a factor of 4 regarding their linear equivalents.

### 3.3. Impact of the degree of branching on the rate constants

The impact of branching on the kinetic data of isomerization of alkyl radicals was discussed by our group [45] for 1,3 and 1,4-H-shift reactions, and we showed that the use of a unique rate coefficient, independent of the degree of branching is not appropriate. Wang et al. [44] proposed general kinetic rates for H-shift reactions based on three aspects: the reactant and product radical nature (primary, secondary or tertiary) and the transition state ring size. These rules were developed from a collection of reactions, a part of them based on minimal structures, with low or no presence of branching in the alkyl chains.

In Figure 10, the rate rules derived by Wang et al. [44] for the isomerization of secondary radicals into secondary radicals (ss) passing through 6-membered ring TS is presented along with rate constants automatically calculated for branched structures in this work.

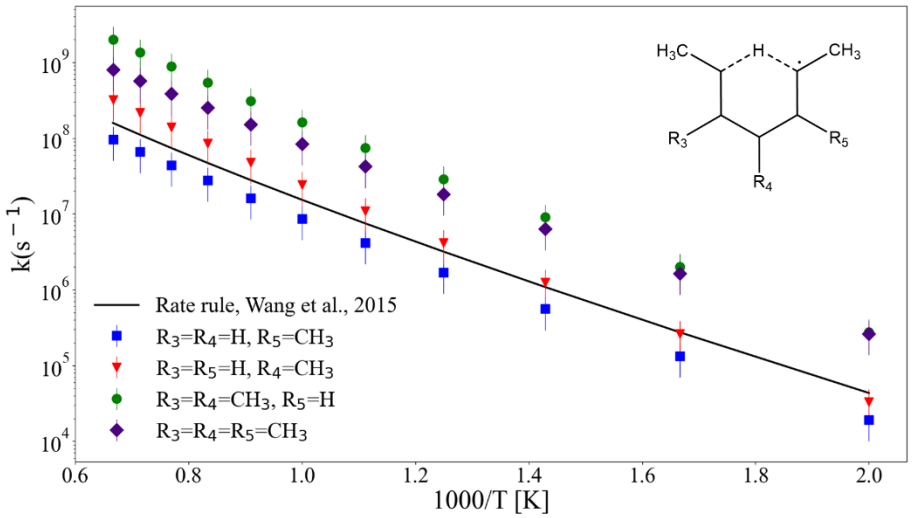


**Figure 10: Rate constants for the isomerization of secondary alkyl radicals into secondary alkyl radicals calculated in this work for multiple branched structures (symbols) and from the rate rule proposed by Wang et al. [44] (solid line).**

It is noticeable that the rate constants increase with the level of branching, and for some cases the increase represents a factor of more than 12 at 1000K compared to the rate rule. In such cases, the use of tabulated transition state models, that explicitly includes the branching level of the alkyl radicals for the definition of the rate rules in reaction mechanisms is preferable for accurate kinetic data.

From the results of the automatic calculations, a table with the Arrhenius parameters for high-pressure limit kinetic rates of all branched structures combinations is available in the Supplemental Material for the 1,5 and 1,2-H-shift reactions in alkyl radicals (S1). These tables, along with the previous ones published by our group [45], cover all the hydrogen migrations in alkyl radicals passing by 3, 4, 5 and 6-membered rings, and includes highly branched structures.

The presence of branching on the alkyl chain highly increases the rate constants from multiple reasons main reasons: the presence of branching in the reactant structure induces gauche interactions that are relaxed in the TS cycle, which decreases the activation energy for more branched structures. For branched chains, the cycle formation may allow the relaxation of the gauche interactions between the substituents on the reactant chain, as the substituents in cyclic structures can be positioned far from each other, as illustrated in Figure S1. This relaxation effect can result in a decrease of the activation energy for branched structures compared to their linear equivalents. At the same time, the pre-exponential factor increases as a consequence of the increase of the number of the increase of the number of transition state configurations, as each TS creates a possible reaction pathway, and the final rate constant is a sum of all the individual ones. Besides, when comparing the ratio between transition state and reactants partition functions, a higher ratio is found for for branched structures, mainly from differences on the vibrational modes, which corroborates to higher rates coefficients for H-shift reactions of branched alkyls. The addition of those behaviours leads to a significant increase on the kinetic rates for branched structures, as observed in Figure 11.

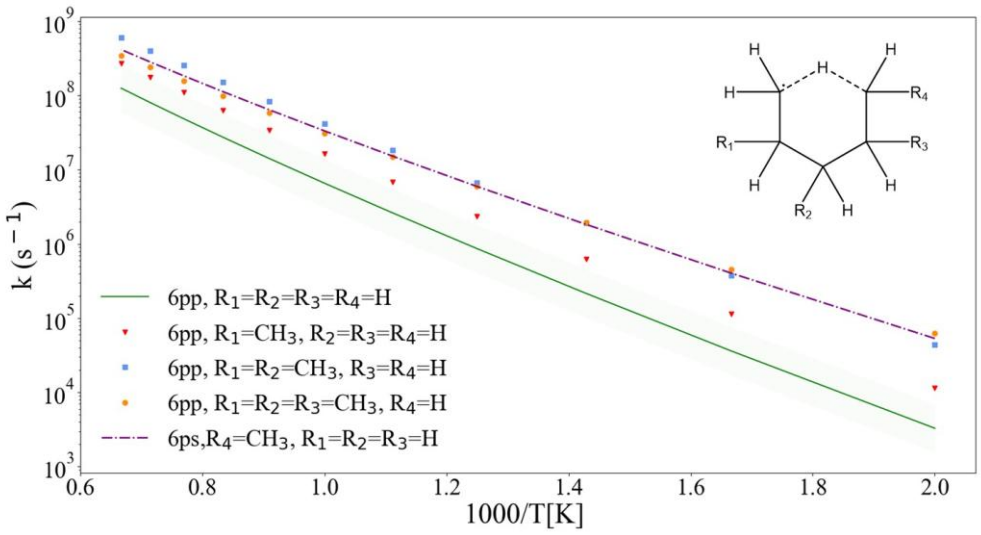


**Figure 11: Rate constants of 6pp and 6ps H-shift reactions for different levels of branching in the carbon chain.**

Besides, when comparing the ratio between transition state and reactants partition functions, a higher ratio is found for branched structures, mainly from differences in the vibrational partition function, which contribute to the higher rates coefficients observed for H-shift reactions in branched alkyls. The ratios between partition functions for the reactions 6pp in linear and branched alkyls are presented in Figure S2, as a function of temperature. The ratio is 6 times higher for the branched alkyl reaction at 500K.

Remarkably, the increase on the kinetic rates produced by the presence of branching on 'spectator' carbon atoms may be in the same range as the increase from changing the nature of the radical formed, as seen in Figure 11: the 6ps rates are close to the 6pp rates for branched structures. In Figure 12, for 6ss and 6st reactions, the increase of rates for

branched structures overcomes the increase from the nature of the reaction (as 6ss reaction in branched structures presents rate constants more than 8 times higher than the 6st in no-branched chain).

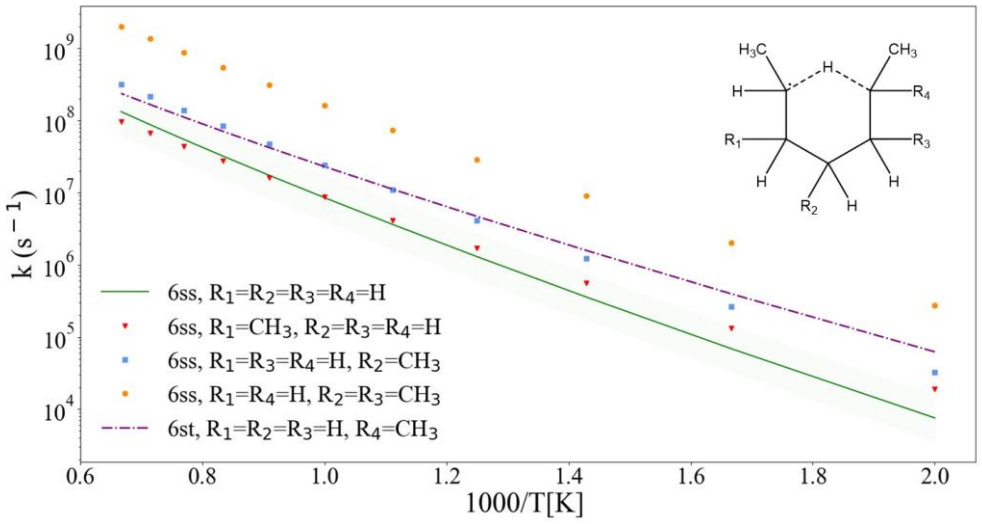


**Figure 12: Rate constants for 6ss and 6st H-shift reactions for different levels of alkyl branching.**

The rate constants of internal H-shift in alkyl chains are mostly impacted by the size of TS cycle, as can be observed in Figure 5. The nature of reactant and product radicals is also considered the second most important aspect influencing the rate coefficient in this reaction class. However, from the results presented in this work, it was observed that the degree of branching and the position of the substituents on the alkyl chain may have a similar impact as the nature of the radicals on the kinetic data. Accounting for this aspect is therefore essential for accurate kinetic data in detailed kinetic mechanism, and for this

purpose, the Tabulated Model of Transition States can be useful for molecular system that are too large for on-the-fly ab initio calculations.

### 3.4. Artifacts induced in kinetic data by the use of methyl to represent alkyl chains

The use of methyl groups to substitute transition state rings imposes not only a given statistical factor L (equation 1), but also a given number of reactants or products and transition states. This count is rigorously correct for the molecular system generated by our code with methyls, but may change if the group represented is an alkyl chain, as the number of optical isomers and symmetries may change if the alkyl chains are different. This complex problem is even more difficult for the most general case of a transition state ring carrying multiple alkyl chains. To illustrate these problems, we first present here two examples for 1,2- and 1-4-H-shift kinetic data generated by our code.

Figure 13 presents a comparison between our results and the ones derived by Wang et al [44] for the modelling of hydrogen atoms reactions with 1 and 2-pentene, theoretically

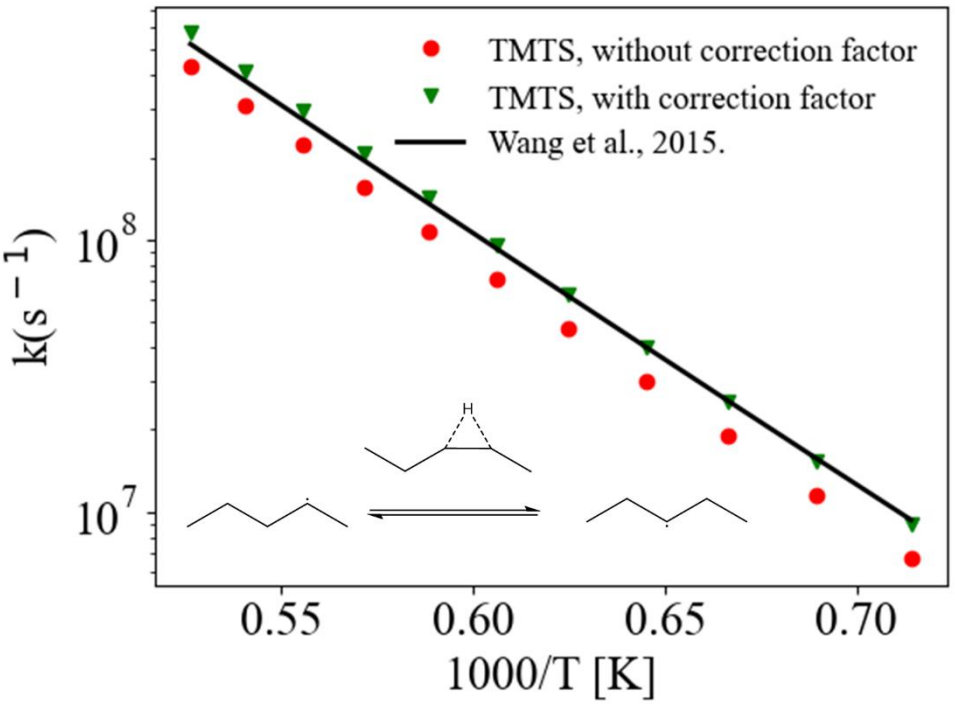

calculated.

**Figure 13: High-pressure limit rate constants of 2-pentyl to 3-pentyl isomerisation calculated based on this work (solid and dotted lines) and from Wang et al**.[44]

Even though the values are close to each other within the estimated errors ( differences of around 40%), the use of methyl as representation of a generic alkyl chain induces a symmetry in the transition state structure. In this specific case, the model reaction used to represent the 2-pentyl -> 3-pentyl radical isomerisation is the 2-butyl -> 2-butyl isomerisation, as illustrated in Figure 14.

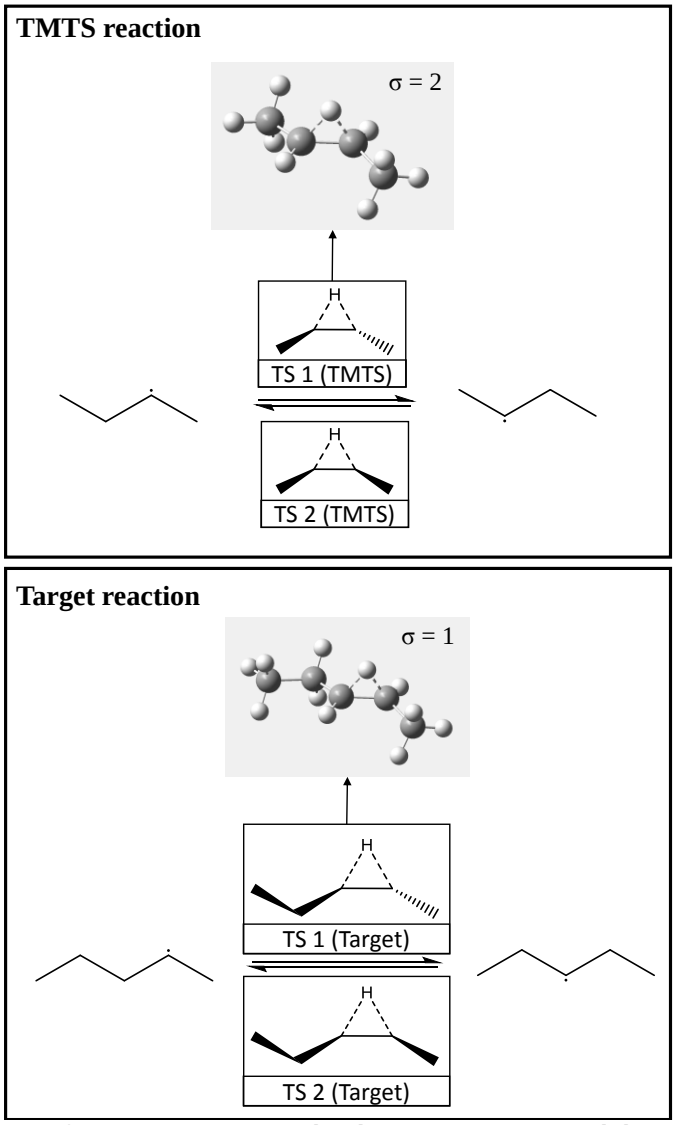


**Figure 14: Differences of structure symmetries between TMTS model reaction and target reaction.**

Both reactions pass by two transition state configurations, depending on the cis/trans positions of the alkyl chain regarding the plane of the 3-membered cycle (trans represented by TS 1 and cis by TS 2 in Figure 14). However, the TS 1 in the TMTS reaction presents an external symmetry of 2 which is not observed for the TS 1 in the reaction of the 2-pentyl radical (called the target reaction).

For other cases, the use of methyl may also change the number of isomers or even the number of available pathways and TS configurations. For those cases, a correction factor for the tabulated transition state rates is necessary, as follow in **(2)**:

$$k_{target} = f_c k_{TMTS} \quad \textbf{(2)}$$

with $k_{target}$ being the kinetic coefficient of the target reaction, $k_{TMTS}$ the kinetic coefficient of the tabulated model transition state reaction and $f_c$ the correction factor.

This factor can be approximated as the ratio between the statistical factor of the target reaction and the model reaction. For the reaction represented in Figure 14, the statistical factor is the same for TS 2 in TMTS and the target reaction, as the symmetries and number of isomers do not change between them. For the TS 1, however, the statistical factor of the TMTS reaction is half of the statistical factor of the target reaction, as the external symmetry changes ($\sigma = 2$ for the TS 1 in the TMTS and $\sigma = 1$ for the TS 1 in the target reaction). Those differences in the statistical factors result in a correction factor of 4/3, considering an equal participation of each pathway. After applying the factor, the kinetic data obtained are closer to the ones proposed by Wang et al. [44], as illustrated by the dotted line in Figure 13 (differences of less than 10%).

For other reactions, the presence of different alkyl chains as substituents can induce new transition state configurations, as illustrated in Figure 15 for a secondary alkyl radical transforming into a tertiary radical passing by a transition state with 5-membered ring. When using two methyl groups as the branching of the tertiary carbon, the equatorial and axial positions in the cyclic TS are equivalent, however if the target reaction presents two

different alkyl chains on these positions, the number of TS configurations is multiplied by 2 as illustrated in the Figure 15.

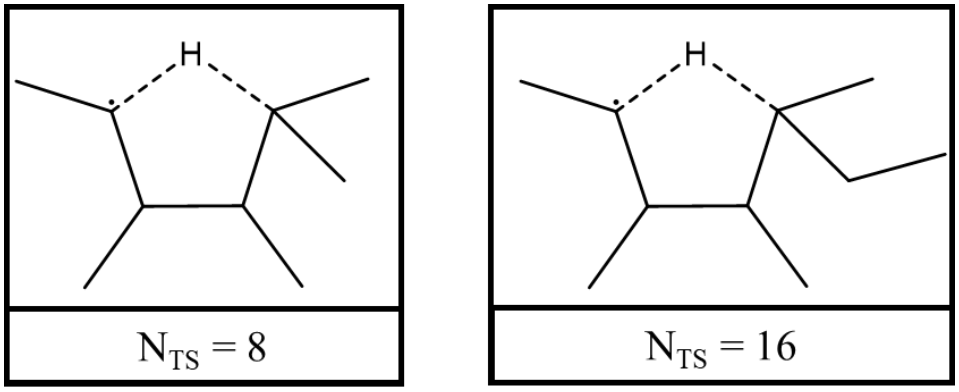


**Figure 15: Number of transition state configuration for a TMTS model reaction and for a target reaction with an ethyl replacing the tertiary carbon methyl.**

For this reaction, the TMTS reaction does not include all the possible reaction pathways due to a symmetry induced by using methyl groups to representant an alkyl groups. However, the use of a correction factor can also be applied by considering that the new arising pathways are equivalent to the ones assigned in the TS model. The rate coefficients of the target reaction of Figure 15 were calculated manually using the same method as previously described, including all the 16 transition state configurations as the combination of equatorial and axial positions by the groups is multiplied by 2. The results for the target reaction were compared with the kinetic data from the TMTS reaction model, with and without the correction factor, as illustrated in **Erreur ! Source du renvoi introuvable.**.

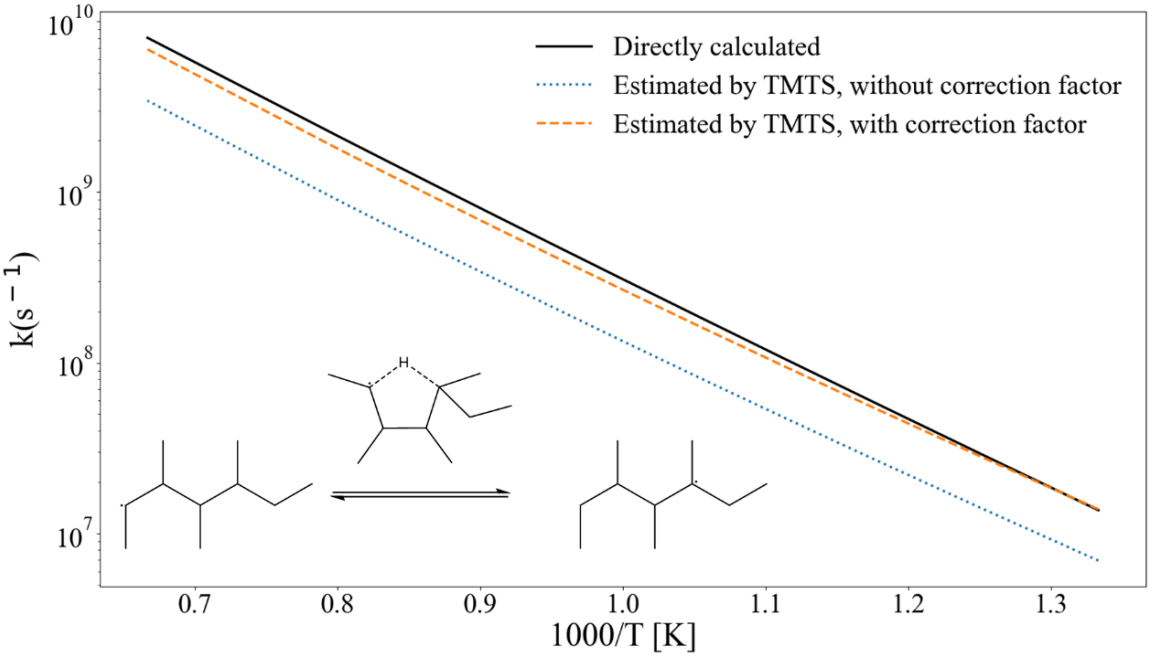


**Figure 16: Rate coefficients calculated for a H-shift in a branched alkyl, directly calculated (16 TS, solid line), estimated by TMTS without using a correction factor (dotted line) and estimated by TMTS including a correction factor (dashed line).**

With no correction factor, the rate constant of the target reaction is underestimated by a factor of 2.3 at 1000 K. If a correction factor defined as the ratio between the number of transition states for each case is used, the rate constant of the target reaction is in good agreement with the complete calculation, with a deviation of less than 20% at 1000 K.

In order to cover the most generic reactions, the tabulated model transition states are presented in the supplemental material with their corresponding statistical factor. For a given target reaction, this statistical factor can be used to calculate and apply the correction factor. The correction factor ($f_c$) can be calculated as the ratio between the statiscal factor of the target reaction and the statiscal factor of the model reaction, as follow:

$$f_c = {L_{Target}}/{L_{TMTS}}$$

In the previous example (illustrated in Figure 15), the $L_{Target}$ is estimated as twice as $L_{TMTS}$, as the number of transition state cconfigurationsis doubled, and the rates for the new pathways created in the target reaction are supposed to be equivalent of the ones in the TMTS model reaction. In the case of Figure 14, $L_{Target}$=2, while $L_{TMTS}$=3/2, which results in $f_c$=4/3. The calculation of this factor is detailed in the supplemental material for generic target reactions. The use of the correction factor in combination with the tabulated models of transition states allows the estimation of kinetic rates for isomerization reactions of branched alkyl radicals with an uncertainty factor of 2.1.

## 4. Conclusions

The code developed in part I of this paper series was applied for the calculation of high-pressure limit rate constants of 1,2-, 1,3- and 1,5-H-shift reactions for a large number of combinations of branched alkyls in the Part I and II of this paper serie. The code creates branched structures based on a minimal non-substituted TS model structure, and performs all the electronic structure and transition state theory calculations, and produces a table of modified Arrhenius coefficients for each branched alkyl isomerisation, with an estimated uncertainty factor of 2.1.

The cyclic transition states involved in these reactions may present different configurations according to the positions of the substituents (equatorial vs. axial positions) and diastereoismers in the reactants / products, which leads to reactions with multiple parallel pathways. The rate constants of isomerizations calculated for hundreds

of reactions by our new code show that it is necessary to take these multiple pathways into account exhaustively to obtain accurate rate coefficients in branched alkyls. It was found that the presence of branching on the chain between the radical carbon and the H-donor carbon can increase the rate constant by factors of more than 10.

The use of methyl groups to represent generic alkyl chain was found to agree with the kinetic data of the literature, however it may induce symmetries, change the number of isomers or even affect the number of available reaction pathways. Since those factors can be isolated from the kinetic rates as a part of the statistical factor, a correction factor for the kinetic rates was proposed to consider those possible changes caused by the use of methyl group to represent an alkyl group. The application of this correction factor was tested for two different reactions – one with loss of symmetry and other with a change in the number of TS configurations. For both cases, the application of the correction factor to correct the tabulated values was enough to reproduce the expected kinetic rates. The tables of transition state models for 1,2-, 1,3 and 1,5-H-shift reactions are provided for all possible branched alkyl isomerizations. Our computed kinetic data for hundreds of H-shifts reactions in alkyls as a function of the degree of branching shows that it is not possible to use a single branching-independent correlation for these reactions. The TMTS method is the only approach able to capture the effect of branching for the rate constants of isomerization, for large alkyl radicals which are still difficult to accurately calculate using on-the-fly ab initio calculations.

**Acknowledgments**

This project has received funding from the European Research Council (ERC) under the European Union's Horizon 2020 research and innovation program (Project: 101003318 - BioSCoPe). High performance computing resources were provided by IDRIS under the allocation AD010812434R1 made by GENCI and also by the EXPLOR center hosted by the University of Lorraine.

## References

[1] A. Demirbas, Political, economic and environmental impacts of biofuels: A review, Appl. Energ. 86 (2009) S108–S117. https://doi.org/10.1016/j.apenergy.2009.04.036.
[2] R.H. Moore, K.L. Thornhill, B. Weinzierl, D. Sauer, E. D'Ascoli, J. Kim, M. Lichtenstern, M. Scheibe, B. Beaton, A.J. Beyersdorf, J. Barrick, D. Bulzan, C.A. Corr, E. Crosbie, T. Jurkat, R. Martin, D. Riddick, M. Shook, G. Slover, C. Voigt, R. White, E. Winstead, R. Yasky, L.D. Ziemba, A. Brown, H. Schlager, B.E. Anderson, Biofuel blending reduces particle emissions from aircraft engines at cruise conditions, Nature 543 (2017) 411–415. https://doi.org/10.1038/nature21420.
[3] Sangeeta, S. Moka, M. Pande, M. Rani, R. Gakhar, M. Sharma, J. Rani, A.N. Bhaskarwar, Alternative fuels: An overview of current trends and scope for future, Renew. Sustain. Energy Rev. 32 (2014) 697–712. https://doi.org/10.1016/j.rser.2014.01.023.
[4] S. Atsumi, T. Hanai, J.C. Liao, Non-fermentative pathways for synthesis of branched-chain higher alcohols as biofuels, Nature 451 (2008) 86–89. https://doi.org/10.1038/nature06450.
[5] G. Knothe, Biodiesel and renewable diesel: A comparison, Prog. Energy Combust. Sci. 36 (2010) 364–373. https://doi.org/10.1016/j.pecs.2009.11.004.
[6] G. Knothe, Improving biodiesel fuel properties by modifying fatty ester composition, Energy Environ. Sci. 2 (2009) 759. https://doi.org/10.1039/b903941d.
[7] S.L. Repetto, J.F. Costello, D. Parmenter, Current and Potential Aviation Additives for Higher Biofuel Blends in Jet A-1, Biofuels for Aviation (2016) 261–275. https://doi.org/10.1016/b978-0-12-804568-8.00011-1.
[8] C.A. Moses, P.N.J. Roets, Properties, Characteristics, and Combustion Performance of Sasol Fully Synthetic Jet Fuel, J. Eng. Gas Turbine. Power 131 (2009). https://doi.org/10.1115/1.3028234.
[9] M.L. Huber, B.L. Smith, L.S. Ott, T.J. Bruno, Surrogate Mixture Model for the Thermophysical Properties of Synthetic Aviation Fuel S-8: Explicit Application of the Advanced Distillation Curve, Energy Fuels 22 (2008) 1104–1114. https://doi.org/10.1021/ef700562c.
[10] P. Oßwald, J. Zinsmeister, T. Kathrotia, M. Alves-Fortunato, V. Burger, R. van der Westhuizen, C. Viljoen, K. Lehto, R. Sallinen, K. Sandberg, M. Aigner, P. Le Clercq, M.

Köhler, Combustion kinetics of alternative jet fuels, Part-I: Experimental flow reactor study, Fuel 302 (2021) 120735. https://doi.org/10.1016/j.fuel.2021.120735.
[11] S. Richter, C. Naumann, U. Riedel, Experimental Study on the Combustion Properties of an Alcohol-to-Jet Fuel, World Congress on Momentum, Heat and Mass Transfer (2017), paper CSP 107. https://doi.org/10.11159/csp17.107.
[12] M. Lapuerta, J.J. Hernández, S.M. Sarathy, Effects of methyl substitution on the auto-ignition of C16 alkanes, Combust. Flame 164 (2016) 259–269. https://doi.org/10.1016/j.combustflame.2015.11.024.
[13] T. Schripp, B. Anderson, E.C. Crosbie, R.H. Moore, F. Herrmann, P. Oßwald, C. Wahl, M. Kapernaum, M. Köhler, P. Le Clercq, B. Rauch, P. Eichler, T. Mikoviny, A. Wisthaler, Impact of Alternative Jet Fuels on Engine Exhaust Composition During the 2015 ECLIF Ground-Based Measurements Campaign, Environ. Sci. Technol. 52 (2018) 4969–4978. https://doi.org/10.1021/acs.est.7b06244.
[14] I. Lee, L.A. Johnson, E.G. Hammond, Use of branched- chain esters to reduce the crystallization temperature of biodiesel, J. Americ. Oil Chem. Soc. 72 (1995) 1155–1160. https://doi.org/10.1007/bf02540982.
[15] K. Bacha, A. Ben-Amara, A. Vannier, M. Alves-Fortunato, M. Nardin, Oxidation Stability of Diesel/Biodiesel Fuels Measured by a PetroOxy Device and Characterization of Oxidation Products, Energy Fuels 29 (2015) 4345–4355. https://doi.org/10.1021/acs.energyfuels.5b00450.
[16] M. Alves-Fortunato, J. Labaume, P. Cologon, L. Barré, Biofuel Surrogate Oxidation: Insoluble Deposits Formation Studied by Small-Angle X-ray Scattering and Small Angle Neutron Scattering, Energy Fuels 32 (2018) 9559–9567. https://doi.org/10.1021/acs.energyfuels.8b02055..
[17] R. Van de Vijver, N.M. Vandewiele, P.L. Bhoorasingh, B.L. Slakman, F. Seyedzadeh Khanshan, H. Carstensen, M. Reyniers, G.B. Marin, R.H. West, K.M. Van Geem, Automatic Mechanism and Kinetic Model Generation for Gas- and Solution- Phase Processes: A Perspective on Best Practices, Recent Advances, and Future Challenges, Int. J. Chem. Kinet. 47 (2015) 199–231. https://doi.org/10.1002/kin.20902.
[18] J.M. Simmie, Detailed chemical kinetic models for the combustion of hydrocarbon fuels, Prog. Energy Combust. Sci. 29 (2003) 599–634. https://doi.org/10.1016/s0360-1285(03)00060-1..
[19] H.J. Curran, P. Gaffuri, W.J. Pitz, C.K. Westbrook, A Comprehensive Modeling Study of n-Heptane Oxidation, Combust. Flame 114 (1998) 149–177. https://doi.org/10.1016/s0010-2180(97)00282-4.
[20] S. Dóbé, T. Bérces, F. Réti, F. Márta, Isomerization of n- hexyl and s- octyl radicals by 1,5 and 1,4 intramolecular hydrogen atom transfer reactions, Int. J. Chem. Kinet. 19 (1987) 895–921. https://doi.org/10.1002/kin.550191003.
[21] M.C. Lin, M.H. Back, The thermal decomposition of ethane: Part III. Secondary reactions, Can. J. Chem. 44 (1966) 2369–2380. https://doi.org/10.1139/v66-358.
[22] A. Miyoshi, J. Widjaja, N. Yamauchi, M. Koshi, H. Matsui, Direct investigations on the thermal unimolecular isomerization reaction of 1-pentyl radicals, Proc. Combust. Inst. 29 (2002) 1285–1293. https://doi.org/10.1016/s1540-7489(02)80158-4.

[23] W. Tsang, J.A. Walker, J.A. Manion, Single-pulse shock-tube study on the decomposition of 1-pentyl radicals, Symp. (Int.) Combust. 27 (1998) 135-142. https://doi.org/10.1016/s0082-0784(98)80398-6
[24] W. Tsang, J.A. Walker, J.A. Manion, The decomposition of normal hexyl radicals, Proc. Combust. Inst. 31 (2007) 141–148. https://doi.org/10.1016/j.proci.2006.07.069.
[25] R.M. Marshall, The rate constant for the intramolecular isomerization of pentyl radicals, Int. J. Chem. Kinet. 22 (1990) 935–950. https://doi.org/10.1002/kin.550220905.
[26] W. Tsang, W.S. McGivern, J.A. Manion, Multichannel decomposition and isomerization of octyl radicals, Proc. Combust. Inst. 32 (2009) 131–138. https://doi.org/10.1016/j.proci.2008.05.048.
[27] E.A. Hardwidge, C.W. Larson, B.S. Rabinovitch, Isomerization of vibrationally excited alkyl radicals by hydrogen atom migration, J. Am. Chem. Soc. 92 (1970) 3278–3283. https://doi.org/10.1021/ja00714a007.
[28] A. Comandini, I.A. Awan, J.A. Manion, Thermal decomposition of 1-pentyl radicals at high pressures and temperatures, Chem. Phys. Lett. 552 (2012) 20–26. https://doi.org/10.1016/j.cplett.2012.09.039.
[29] J.A. Manion, I.A. Awan, The decomposition of 2-pentyl and 3-pentyl radicals, Proc. Combust. Inst. 34 (2013) 537–545. https://doi.org/10.1016/j.proci.2012.05.078.
[30] K.W. Watkins, L.A. Ostreko, Isomerization of n-hexyl radicals in the gas phase, J. Phys. Chem. 73 (1969) 2080–2083. https://doi.org/10.1021/j100726a080.
[31] W. Tsang, I.A. Awan, J.A. Manion, Multichannel Decomposition of Heptyl Radicals, *Proceedings of the Third Joint Meeting of the U.S. Sections of the Combustion Institute* (2003).
[32] W.S. McGivern, I.A. Awan, W. Tsang, J.A. Manion, Isomerization and Decomposition Reactions in the Pyrolysis of Branched Hydrocarbons: 4-Methyl-1-pentyl Radical, J. Phys. Chem. A 112 (2008) 6908–6917. https://doi.org/10.1021/jp8020003.
[33] I.A. Awan, W.S. McGivern, W. Tsang, J.A. Manion, Decomposition and Isomerization of 5-Methylhex-1-yl Radical, J. Phys. Chem. A 114 (2010) 7832–7846. https://doi.org/10.1021/jp102313p.
[34] L.C. Jitariu, L.D. Jones, S.H. Robertson, M.J. Pilling, I.H. Hillier, Thermal Rate Coefficients via Variational Transition State Theory for the Unimolecular Decomposition/Isomerization of 1-Pentyl Radical: Ab Initio and Direct Dynamics Calculations, J. Phys. Chem. A 107 (2003) 8607–8617. https://doi.org/10.1021/jp034843z.
[35] F. Wang, D.B. Cao, G. Liu, J. Ren, Y.W. Li, Theoretical study of the competitive decomposition and isomerization of 1-hexyl radical, Theor. Chem. Acc. 126 (2009) 87–98. https://doi.org/10.1007/s00214-009-0685-y
[36] B. Viskolcz, G. Lendvay, T. Körtvélyesi, L. Seres, Intramolecular H Atom Transfer Reactions in Alkyl Radicals and the Ring Strain Energy in the Transition Structure, J. Am. Chem. Soc. 118 (1996) 3006–3009. https://doi.org/10.1021/ja951393i.
[37] A. Ratkiewicz, B. Bankiewicz, T.N. Truong, Kinetics of thermoneutral intermolecular hydrogen migration in alkyl radicals, Phys. Chem. Chem. Phys. 12 (2010) 10988. https://doi.org/10.1039/c0cp00293c.
[38] J. Power, K.P. Somers, C.-W. Zhou, S. Peukert, H.J. Curran, Theoretical, Experimental, and Modeling Study of the Reaction of Hydrogen Atoms with 1- and 2-

Pentene, J. Phys. Chem. A 123 (2019) 8506–8526. https://doi.org/10.1021/acs.jpca.9b06378.
[39] B. Sirjean, E. Dames, H. Wang, W. Tsang, Tunneling in Hydrogen-Transfer Isomerization of n-Alkyl Radicals, J. Phys. Chem. A 116 (2011) 319–332. https://doi.org/10.1021/jp209360u..
[40] A.C. Davis, J.S. Francisco, Ab Initio Study of Hydrogen Migration across n-Alkyl Radicals, J. Phys. Chem. A 115 (2011) 2966–2977. https://doi.org/10.1021/jp110142.
[41] A.C. Davis, J.S. Francisco, Ab Initio Study of Key Branching Reactions in Biodiesel and Fischer–Tropsch Fuels, J. Am. Chem. Soc. 133 (2011) 19110–19124. https://doi.org/10.1021/ja205516s.
[42] A.C. Davis, J.S. Francisco, Ab initio study of chain branching reactions involving second generation products in hydrocarboncombustion mechanisms, Phys. Chem. Chem. Phys. 14 (2012) 1343–1351. https://doi.org/10.1039/c1cp22602a.
[43] K. Wang, S.M. Villano, A.M. Dean, Reactivity–Structure-Based Rate Estimation Rules for Alkyl Radical H Atom Shift and Alkenyl Radical Cycloaddition Reactions, J. Phys. Chem. A 119 (2015) 7205–7221. https://doi.org/10.1021/jp511017z.
[44] F. Citrangolo Destro, R. Fournet, V. Warth, P.-A. Glaude, B. Sirjean, Impact of the size and degree of branching of alkanes on the rate rules approach: The case of isomerizations, Proc. Combust. Inst. 39 (2023) 611–620. https://doi.org/10.1016/j.proci.2022.07.170.
[45] S.J. Klippenstein, L.B. Harding, B. Ruscic, Ab Initio Computations and Active Thermochemical Tables Hand in Hand: Heats of Formation of Core Combustion Species, J. Phys. Chem. A 121 (2017) 6580–6602. https://doi.org/10.1021/acs.jpca.7b05945.
[46] A.S. Hansen, T. Bhagde, K.B. Moore III, D.R. Moberg, A.W. Jasper, Y. Georgievskii, M.F. Vansco, S.J. Klippenstein, M.I. Lester, Watching a hydroperoxyalkyl radical (•QOOH) dissociate, Science 373 (2021) 679–682. https://doi.org/10.1126/science.abj0412.
[47] J.C. Lizardo-Huerta, B. Sirjean, R. Bounaceur, R. Fournet, Intramolecular effects on the kinetics of unimolecular reactions of β-HOROO˙ and HOQ˙OOH radicals, Phys. Chem. Chem. Phys. 18 (2016) 12231–12251. https://doi.org/10.1039/c6cp00111d.
[48] A.C. Davis, J.S. Francisco, Ab initio study of chain branching reactions involving second generation products in hydrocarboncombustion mechanisms, Phys. Chem. Chem. Phys. 14 (2012) 1343–1351. https://doi.org/10.1039/c1cp22602a.